Development of multigroup cross section library generation system TPAMS

Lili Wen[1], Haicheng Wu[*1], Xiaoming Chai[2], Ying Chen[*1], Xiaofei Wu[1], Xiaolan Tu[2], Yuan Liu[2]

(1. China Institute of Atomic Energy, China Nuclear Data Center, Beijing 102413, China;

2. Nuclear Power Institute of China, Chengdu 610041, China)

[*] Corresponding author: haicheng@ciae.ac.cn, cying_1204@163.com

1. Introduction

An advanced neutronics lattice code called KYLIN-2 has been developed by Nuclear Power Institute of China to simulate assembly of current pressurized water reactor and advanced reactor [1-3]. The KYLIN-2 code has various capabilities such as resonance treatment as well as transport and burnup calculation, thus the KYLIN-2 code requires a multi-group library which contains resonance parameters, transport cross section and bumup data to support all its simulation capabilities. The key characteristics of KYLIN-2 code include the subgroup method for resonance treatment; the method of characteristics (MOC) for transport calculation and the Chebyshev rational approximation method (CRAM) for depletion calculation. Accordingly, subgroup parameters are need for the code, depletion chain is also necessary. Considering the balance between computational accuracy and efficiency of KYLIN-2, the fine depletion chain including thousands of nuclides is unrealistic. It is necessary to simplify the depletion chain especially for the thousands of fission product nuclides.

The methods for generating subgroup parameters mainly include fitting [4] and moment method[5], fitting method directly using the effective resonance integral table to fit the subgroup parameters, and the moment method using the "moment" of the real section to generate subgroup parameters. However, both methods involve the process of numerical optimization and fitting, and the resulting subgroup parameters have the phenomenon of subgroup cross-section with 0 value, subgroup weight with negative value, etc., and the stability of subgroup parameters is still a problem. Common depletion chain simplification methods include WLUP method[6], contribution matrix method[7], singular value

decomposition method[8], contribution function method[9], and quantitative importance analysis method[10]. These methods have their own advantages and disadvantages, but it is difficult to apply them to the depletion chain compression for KYLIN-2.

In order to make a multigroup cross section library for KYLIN-2 and overcome the above problems, we develop a multigroup constant library production system TPAMS (**TPA**X format **M**ultigroup library production **S**ystem), in which in addition to the least squares fitting method to generate subgroup parameters, a subgroup parameters calculation module based on differential evolution algorithm[11] is also developed. Aiming at the compression of the fission product depletion chain, a quantitative compression method is proposed and the corresponding fission product depletion chain compression module is developed in TPAMS. In addition, for other resonance data other than subgroup parameters, such as intermediate resonance factors and resonance integrals, corresponding calculation modules have been developed, TPAMS can calculate intermediate resonance factors that vary with the energy group, homogeneous and heterogeneous resonance integrals.

In this paper the above methods of TPAMS will be described in detail, and in order to verify the reliability of TPAMS, a multigroup cross section library with 45 neutron energy groups and 18 photon groups was produced based on TPAMS, and the reliability of TPAMS is verified to a certain extent by the critical and burnup benchmarking of the multigroup cross section library.

2. Methods in TPAMS

2.1 Subgroup parameters fitting

In the homogeneous problems, the relationship between absorption resonance integral and the subgroup parameters is showed as Equation (1):

$$R_l = \sum_{n=1}^{N} \frac{\omega_n}{\left(\sigma_n\right)^{-1} + \left(\sigma_{0,l}\right)^{-1}} \qquad (1)$$

where the subscript n represents the ordinal number of the subgroup, σ_n is subgroup cross section, and ω_n is subgroup probability (also known as subgroup weight). The subgroup cross section and subgroup probability are collectively referred to as subgroup

parameters, and in the subgroup method, the subgroup parameters need to be calculated in advance by the fitting method to solve the subgroup transport equation. Based on Equation (1), the subgroup parameters can be obtained using the least squares fitting method, as showed in Equation (2).

$$\min F\left(\omega_n,\sigma_n\right)=\sum_{l=1}^{L}\left[1-\frac{1}{R_l}\sum_{n=1}^{N}\frac{\omega_n}{\left(\sigma_n\right)^{-1}+\left(\sigma_{b,l}\right)^{-1}}\right]^2 \tag{2}$$

Negative subgroup parameters sometimes occur when fitting subgroup parameters, especially negative subgroup cross sections, which cause many difficulties in solving the subgroup transport equation. In order to avoid negative subgroup parameters, it is necessary to introduce certain constraints to Equation (2) to ensure that the subgroup probability is positive, the subgroup cross section is positive, and the sum of the subgroup probabilities is 1. To deal with the fitting problem with constraints, the penalty function method is used to transform a constrained problem into an unconstrained penalty function problem. In addition, according to the requirements of KYLIN-2, the same set of subgroup cross sections is used at different temperature points of the same resonance nuclide, and the subgroup probability varies with different temperatures, so it is necessary to uniformly fit the subgroup parameters at all temperature points, and the corresponding minimum problem is Equation (3):

$$\begin{aligned}\min F\left(\omega_n,\sigma_n\right)&=\sum_{l=1}^{L}\sum_{t=1}^{T}C_l^t\left[1-\frac{1}{R_l^t}\sum_{n=1}^{N}\frac{\omega_n^t}{\left(\sigma_n\right)^{-1}+\left(\sigma_{b,l}\right)^{-1}}\right]^2+C_{L+1}P\left(\omega_n^t,\sigma_n\right)\\ P\left(\omega_n^t,\sigma_n\right)&=\left[\sum_{n=1}^{N}2(1-e^{\sigma_n})+\sum_{t=1}^{T}\sum_{n=1}^{N}2(1-e^{\omega_n^t})+\sum_{t=1}^{T}2(1-e^{-\left|1-\sum_{n=1}^{N}\omega_n^t\right|})\right]^2\end{aligned} \tag{3}$$

The penalty function $P\left(\omega_n^t,\sigma_n\right)$ in the equation is the penalty term for the objective function of an optimization problem.

On the other hand, according to the relationship between the resonance integral and the subgroup parameters, under the condition of infinite dilution, the background cross section tends to infinity, and the flux is infinitely close to 1, so there are constraints as shown in Equation (4):

$$R_{l,\infty}=\lim_{\sigma_{b,l}\to\infty}\sum_{n=1}^{N}\sigma_n\omega_n\frac{\sigma_{b,l}}{\sigma_{n,a}+\sigma_{b,l}}=\sum_{n=1}^{N}\sigma_n\omega_n \tag{4}$$

Constraining equation (4) in the form of a penalty function, the final fitting formula for the subgroup parameters is as follows:

$$\min F\left(\omega_n,\sigma_n\right)=\sum_{l=1}^{L}\sum_{t=1}^{T}C_l^t\left[1-\frac{1}{R_l^t}\sum_{n=1}^{N}\frac{\omega_n^t}{\left(\sigma_n\right)^{-1}+\left(\sigma_{b,l}\right)^{-1}}\right]^2+C_{L+1}P\left(\omega_n^t,\sigma_n\right)$$

$$P\left(\omega_n^t,\sigma_n\right)=\left[\sum_{n=1}^{N}(1-e^{\sigma_n})+\sum_{t=1}^{T}\sum_{n=1}^{N}(1-e^{\omega_n^t})+\sum_{t=1}^{T}(1-e^{-\left|1-\sum_{n=1}^{N}\omega_n^t\right|})+\sum_{t=1}^{T}(1-e^{-\left|1-\frac{\sum_{n=1}^{N}\sigma_{n,a}\omega_{n,a}^t}{R_\infty}\right|})\right]^2 \quad (5)$$

When calculating the subgroup parameters based on the least squares fitting method, the Levenberg-Marquardt algorithm is used to solve the nonlinear minimum problem showed as Equation (5), and the Jacobi matrix is calculated by the finite difference method. But as mentioned earlier, the stability of the fit is still a difficult problem. Therefore, the differential evolution algorithm is used as a supplement to the least squares method, and the subgroup parameter fitting method based on the differential evolution algorithm is added to TPAMS.

As the subgroup parameters need to meet the following constraints: the value range of the subgroup probability is 0-1, the sum of all subgroup probabilities is 1, the subgroup cross section must be positive, the maximum subgroup cross section cannot exceed the maximum group cross section, the orthogonal product of the subgroup cross section and subgroup probability is the same as the infinite dilution resonance integral. Accordingly, when fitting subgroup parameters based on the differential evolution algorithm, it is necessary to initialize the parameters of all individuals in the population sequentially according to the above constraints at the initialization stage, and the initialization method is as follows:

$$\omega_{i,j}^0=1-\sum_{s=1}^{N-1}\omega_{i,s}^0,\ j=N \quad (6)$$

$$\omega_{i,j}^0\in\left(0,1-\sum_{s=1}^{j-1}\omega_{i,s}^0\right),\ j\le N-1 \quad (7)$$

$$\sigma_{i,j}^0=\sigma_{i,j}^L+rand(0,1)\times\left(\sigma_{i,j}^H-\sigma_{i,j}^L\right) \quad (8)$$

where i represents the i-th individual of the NP individuals, j represents the j-dimension of the i-th individual (the maximum number of j is the subgroup order N), and $\sigma_{i,j}^L$ is the lower and $\sigma_{i,j}^H$ upper bounds of the j-th dimension, respectively.

First, the absorption subgroup parameters are calculated, and then the fission production subgroup parameters, and the fitting adaptation functions of absorption and fission production subgroup parameters are shown in Equation (9) and Equation (10), respectively:

$$\min F\left(\omega_{n,a}^{t},\sigma_{n,a}\right)=\max\left|C_{a,l}^{t}\left[1-\frac{1}{R_{a,l}^{t}}\sum_{n=1}^{N}\frac{\omega_{n,a}^{t}}{\left(\sigma_{n,a}\right)^{-1}+\left(\sigma_{b,l}\right)^{-1}}\right]\right| \tag{9}$$

$$\min F\left(\omega_{n,a}^{t},\sigma_{n,a},\omega_{n,\mathrm{f}}^{t},\sigma_{n,\mathrm{f}}\right)=\max\left|C_{\mathrm{f},l}^{t}\left(1-\frac{R_{a,l}^{t}}{R_{\mathrm{f},l}^{t}}\frac{\sum_{n=1}^{N}\frac{\sigma_{n,\mathrm{f}}\omega_{n,\mathrm{f}}^{t}\sigma_{b,l}}{\sigma_{n,\mathrm{a}}+\sigma_{b,l}}}{\sum_{n=1}^{N}\frac{\omega_{n,\mathrm{a}}^{t}}{\left(\sigma_{n,a}\right)^{-1}+\left(\sigma_{b,l}\right)^{-1}}}\right)\right| \tag{10}$$

2.2 intermediate resonance factor

The intermediate resonance factor is a measure of the energy lost in an elastic collision of a neutron with a target nucleus relative to the width of the resonance peak of the main resonance nuclide. The smaller the mass of the target nucleus, the greater the energy loss, the narrower the resonance peak relatively, thus close to the assumption of the narrow resonance approximation, and the intermediate resonance factor is close to 1. The greater the mass of the target nucleus, the smaller the energy loss, the wider the resonance peak relatively, thus close to the assumption of the wide resonance approximation, and the intermediate resonance factor is close to 0. The width of the resonance peak is different in each energy group, so the intermediate resonance factor varies with the energy group. The energy group dependent intermediate resonance factor is calculated as follows:

（1） Selecting the main resonance nuclide R, and a series of homogeneous problems of the resonance nuclide R and hydrogen are calculated, in which the number density of R remains unchanged and the number density of hydrogen is changed. Assuming that the intermediate resonance factor of the resonant nuclide R λ_{r} is known, a list matrix between the effective section σ_a and the background section σ_b can be constructed:

$$\sigma_{a,j}=f\left(\sigma_{\mathrm{b},j}\right) \tag{11}$$

where the subscript j indicates the jth homogeneous problem.

$$\sigma_{b,j}=\lambda_r\sigma_{p,r}+{\sigma_{p,h}N_{h,j}}\Big/{N_r} \tag{12}$$

σ_b is background cross section, σ_p is potential scattering cross section, N is nuclide number

density.

（2） For nuclide X, which requires the calculation of intermediate resonance factors, calculating a homogeneous problem including resonance nuclide R, hydrogen and X, and the effective absorption cross section $\sigma_{a,x}$ is obtained.

（3） By interpolating in the list between the effective cross section σ_a and the background cross section σ_b, the background cross section $\sigma_{b,x}$ corresponding to the effective absorption cross section $\sigma_{a,x}$ is obtained.

（4） The intermediate resonance factor of nuclide X is calculated by Equation (13):

$$\lambda_x = \frac{\sigma_{b,x} - l_r\sigma_{p,r} - \sigma_{p,h}N_h / N_r}{\sigma_{p,x}N_x / N_r} \tag{13}$$

2.3 resonance integrals

The homogeneous resonance integral is calculated by Equation (14).

$$\frac{IR_{\mathrm{x},g}}{\Delta u_g} = \frac{\sigma_{\mathrm{x},g}\sigma_{\mathrm{b}}}{\sigma_{\mathrm{a},g} + \sigma_{\mathrm{b}} + \lambda\sigma_{s,\mathrm{r},g}} \tag{14}$$

where $IR_{\mathrm{x},g}$ is the resonance integral of the reaction x in energy group g, and $\sigma_{\mathrm{x},g}$ the cross section of the x reaction in energy group g, σ_{b} is the background cross section, Δu_g is the lethargy width of energy group g.

The calculation of the heterogeneous resonance integral requires the construction of a series of different problems, which are calculated by the MC code to obtain the multi-group cross section in the fuel. The calculated multi-group cross section then is used to solve the fixed source for the above different problems, and the fixed source equation solved is as follows:

$$\Omega\cdot\nabla\phi_g(r,\Omega) + (\Sigma_{a,g}(r) + \lambda\Sigma_p(r))\phi_g(r,\Omega) = \frac{\Delta u_g\lambda\Sigma_p(r)}{4\pi} \tag{15}$$

The average flux in the fuel calculated by equation (15) and the multi-group cross section calculated by MC are substituted into equation (16), (17) to obtain the escape section Σ_e and background cross section σ_b.

$$\Sigma_e = \frac{(\Sigma_{a,f,g} + \lambda\Sigma_{s,f,g})\phi_{f,g}}{\Delta u_g - \phi_{f,g}} \tag{16}$$

$$\sigma_b = (\lambda\Sigma_{p,f} + \Sigma_e) / N_r \tag{17}$$

The background cross section and multi-group cross section are obtained, and then the heterogeneous resonance integral table is calculated by Equation (14).

2.4 fission product depletion chain compression

According to the transmutation trajectory analysis (TTA) method[12], the concentration $N_n(t)$ for the nth linear nuclide in a chain at the end of the time interval t as follow:

$$N_n(t) = \sum_{m=1}^{n} \frac{1}{\alpha_n \gamma_n} \prod_{k=m}^{n} \alpha_k \gamma_k \left\{ \overline{y_m s} \left[\frac{1}{\prod_{l=m}^{n} \beta_l} - \sum_{j=m}^{n} \frac{\exp(-\beta_j t)}{\beta_j \prod_{i=m, i\neq j}^{n} (\beta_i - \beta_j)} \right] + N_m(0) \sum_{j=m}^{n} \frac{\exp(-\beta_j t)}{\prod_{i=m, i\neq j}^{n} (\beta_i - \beta_j)} \right\} \tag{18}$$

Where $N_m(0)$ is concentration of the mth nuclide at the initial time, β_i is the total transmutation probability of nuclide i

$$\beta_i = \lambda_i + \int_E \phi \sigma_a^i \tag{19}$$

Here λ_i is the decay constant of the ith nuclide.

For fission products, assuming $N_m(0) = 0$ at the initial time, then the concentration of fission products in the initial state without fission products can be obtained as follow:

$$N_n(t) = \sum_{m=1}^{n} \frac{1}{\alpha_n \gamma_n} \prod_{k=m}^{n} \alpha_k \gamma_k \left\{ \overline{y_m s} \left[\frac{1}{\prod_{l=m}^{n} \beta_l} - \sum_{j=m}^{n} \frac{\exp(-\beta_j t)}{\beta_j \prod_{i=m, i\neq j}^{n} (\beta_i - \beta_j)} \right] \right\} \tag{20}$$

If only one fission nuclide is considered, then

$$N(t) = N_f(t)\left[1 - \exp(-\beta t)\right] \int \frac{y(E)}{\beta} \sigma_f(E) \phi(E) dE = N_f(t) \int y_{eff}(E, t) \sigma_f(E) \phi(E) dE \tag{21}$$

Where, $y_{eff}(E, t)$ can be regarded as the effective fission yield which defined in Equation (22).

$$y_{eff}(E,\ t) = y(E) \frac{1 - \exp(-\beta t)}{\beta} \tag{22}$$

According to Equation (21), N(t) is proportional to $y_{eff}(E,t)$, such two contribution functions for fission product depletion chain simplification can be constructed as follow:

(1) Effective fission yield as showed in Equation (22)

(2) Contribution of fission product (absorption reaction) to total reactivity in depletion step interval $T_{\min}$

$$R=\int_{t=0}^{T_{\min}} N(t)\sigma_a\phi dt=\int_{t=0}^{T_{\min}} \sigma_a\phi\left\{N_f(t)\left[1-\exp(-\beta t)\right]\int \frac{y(E)}{\lambda+\sigma_a\phi}\sigma_f(E)\phi(E)dE\right\}dt \qquad (23)$$

The importance of each fission product can be ranked by the quantitative calculation of these two contribution functions, so as to select the important nuclides and achieve the purpose of fission product depletion chain compression.

3. Development of TPAMS

3.1 organizational structure

TPAMS system includes an online input parameter library, driver, data processing program, and test program. The online input parameter library contains the effective fission yield associated with the depletion chain, the decay data extracted from the decay database, and the resulting user parameters (e.g. intermediate resonance factor, heterogeneous resonance integral, etc.) that are set or calculated uniformly according to the needs of the data processing process. The driver uses a full set of neutron data, fission yield database and decay database, and online input parameter library as input to generate input cards for data processing procedures, batch files, etc. Data processing program include NJOY[13], format conversion interface, subgroup parameter fitting module, working library generation module, energy group collapsing module, base conversion module, etc. The test program includes a cross section self-consistency and plausibility check module and a defect test module.

3.2 procedure for generating library

The procedure of generating multi-group cross section library based on TPAMS is shown in Figure 1. The driver preTPEXR of the TPAMS system reads the user input parameters, decay constant table and effective fission yield from the input parameter library InPar, neutron evaluated data from the evaluated nuclear data file, and then generates the input cards

required by data processing code NJOY and format conversion module TPEXR, batch script is generated at the same time. Run the batch script to perform NJOY processing and TPEXR processing successively, and you can complete the production of the multi-group cross section file without subgroup parameters for single nuclide. Then the subgroup parameter fitting module is called to fit the subgroup parameters, a data processing module named ADDSUB is used to merge the subgroup parameters into each single nuclide data file containing resonance nuclide. Finally, the working library generation module is used to combine the single nuclide data files into a working library that can be directly applied by KYLIN-2.

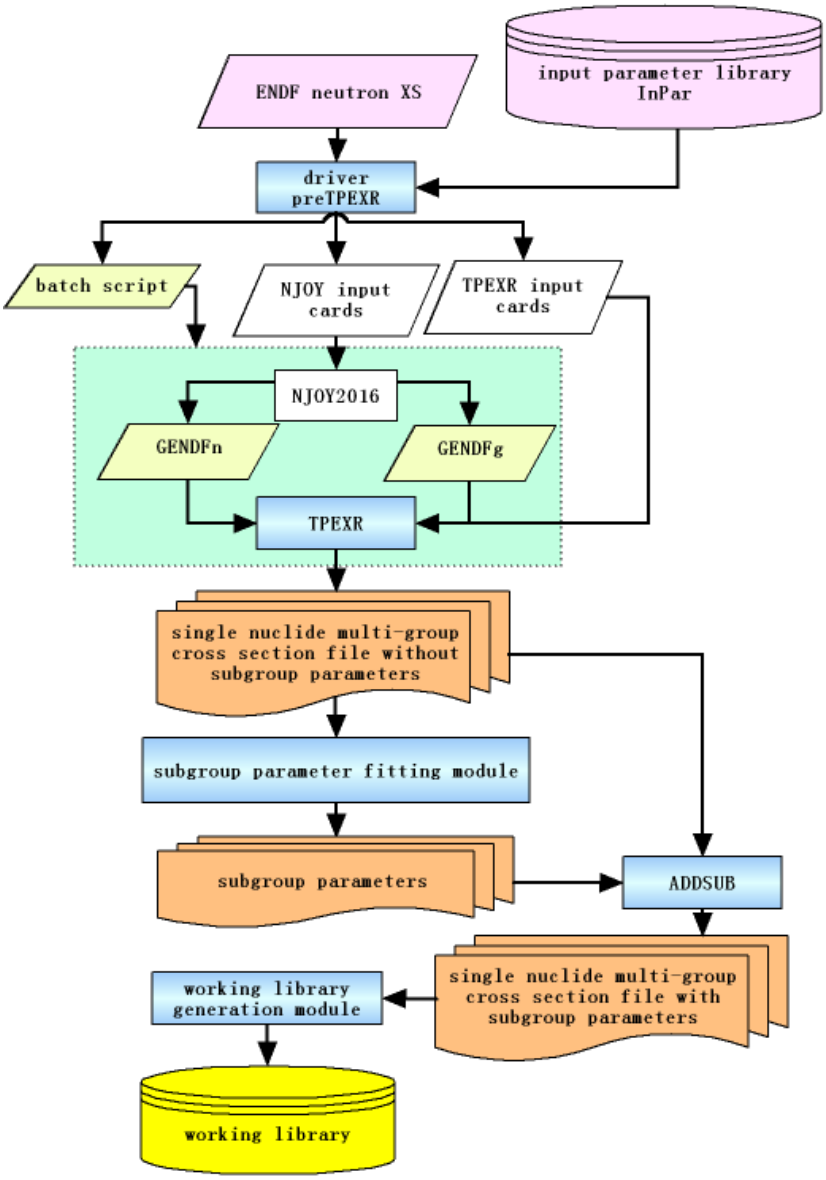

Figure 1 procedure of generating multi-group cross section library based on TPAMS

4. Library generation and benchmark calculation

4.1 library generation

The multi-group cross section library CENP-45 was generated based on the evaluation nuclear database CENDL-NP-1.3 by TPAMS, the decay data was from Nudat[14], and the effective fission yield was calculated based on ENDF/B-VII.1[15]. The thermal scattering law data were used from the ENDF/B-VII.1 library, and the thermal scattering law for light water were evaluated by the CAB laboratory in Argentina.

The multi-group cross section library was generated in 45 neutron energy groups, 18 gamma energy groups, and contains 415 nuclides. For non-moderator materials, the nuclide temperature is 293K, 600K, 900K, 1200K, 1500K, 1800K, 2100K, 2500K. For thermal scattering materials, the temperature grid is the same as the thermal scattering law file. The background cross section grid for resonance integral contains 16 and 32 background cross section points, and the P5 scattering data is given in the library.

4.2 criticality benchmark

Criticality benchmark calculations have been performed for 6 fast spectrum experiments and 51 thermal spectrum experiments from ICSBEP[16]. The k_{eff} or k_{inf} are calculated for all these benchmark experiments and compared with experiment values, The results of fast spectrum experiments are showed in Table 1, results of thermal spectrum experiments are showed in Figure 2-Figure 7.

Table 1 benchmark calculation results of fast spectrum experiments

identifier	EALF(MeV)	C/E of k_{eff}
Godiva	0.881	1.0028
HCI4.1	1.32E-4	0.9952
Jezebel	1.33	0.9957
Jezebel-Pu	1.33	0.9946
PCI1.1	3.19E-4	0.9987
Jezebel-233	1.12	0.9985

For the fast spectrum experiments, the deviation of C/E (ratio of calculated result to experiment value) values for k_{inf} is between 282pcm to -538pcm, the variance is 0.79.

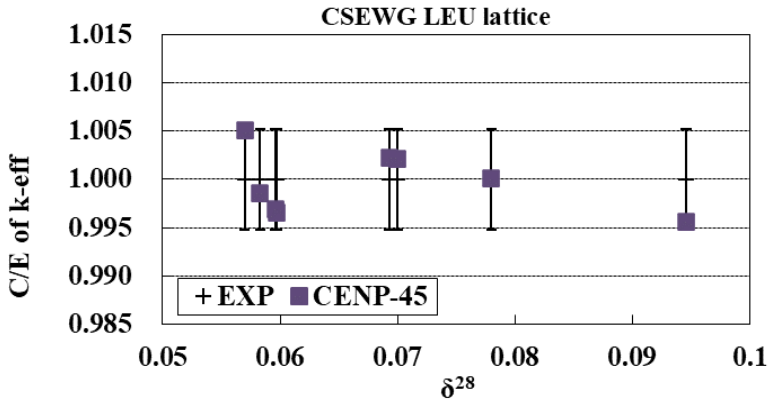

Figure 2 benchmark calculation results of CSEWG LEU lattice

For the CSEWG low enrichment uranium lattice experiments (which include TRX-1,TRX-2,MIT-1,MIT-2,MIT-3,BAPL-1,BAPL-2,BAPL-3), the deviation of C/E (ratio of calculated result to experiment value) values for k_{eff} differ from -440pcm to 510pcm, the variance is 0.21.

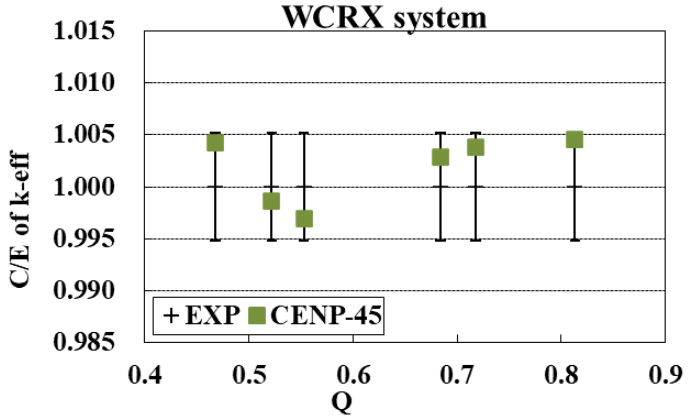

Figure 3 benchmark calculation results of WCRX system

For the WCRX system (which include MOX fuel lattices WCRX-pu1,2,3,4,5,6), the deviation of C/E values for k_{eff} differ from -300pcm to 460pcm, the variance is 0.87.

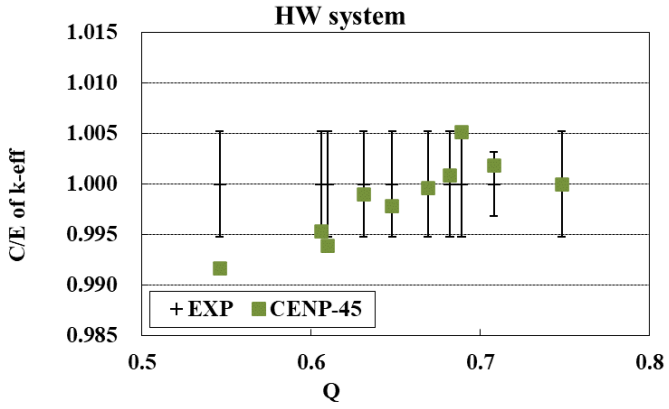

Figure 4 benchmark calculation results of HW system

For the HW system (which include metal uranium fuel lattices HWuma1,2,3,4 and HWUMB1,2,3,4,5,6), the deviation of C/E values for k_{eff} differ from -800pcm to 500pcm, the average difference is 306pcm.

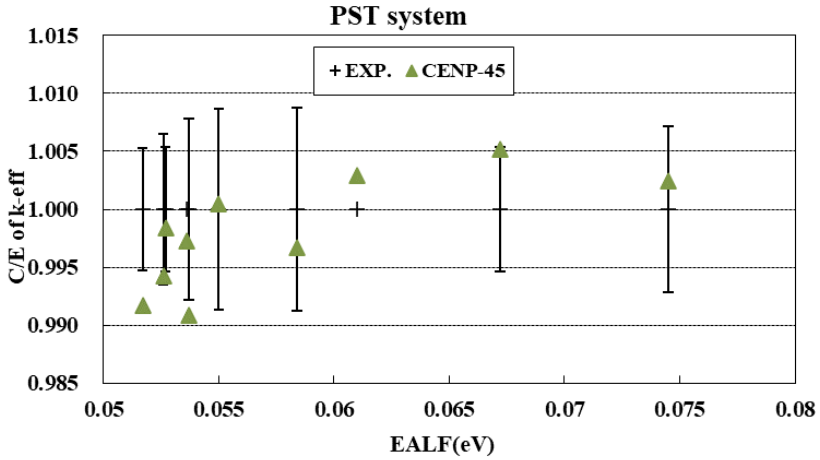

Figure 5 benchmark calculation results of PST system

For the PST (plutonium solution experiment) system, when EALF is in the range of 0.05 to 0.075 eV, the deviation of C/E results differ from -1148pcm to 366pcm.

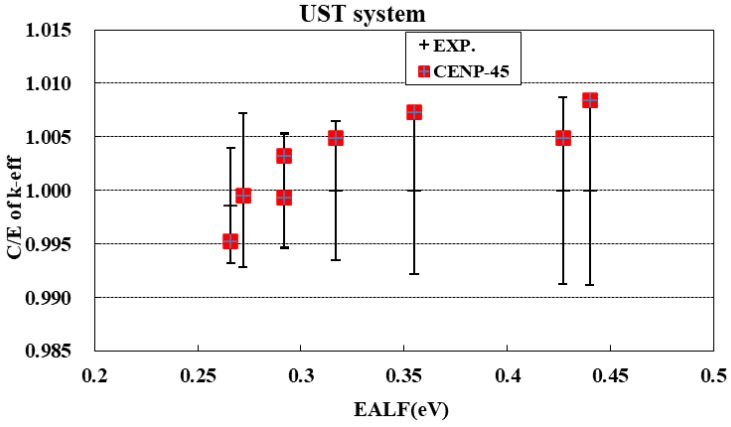

Figure 6 benchmark calculation results of UST system (EALF is in the range of 0.025 to 0.05eV)

For the UST system (uranium solution experiment), when EALF is in the range of

0.025eV to 0.05eV, the deviation of C/E results differ from -123pcm to 1178pcm. When EALF is in the range of 0.055 to 0.085eV, the deviation of C/E results differ from 63pcm to 665pcm; when EALF is in the range of 0.25 to 0.45 eV, the deviation of C/E results differ from -479pcm to 843pcm.

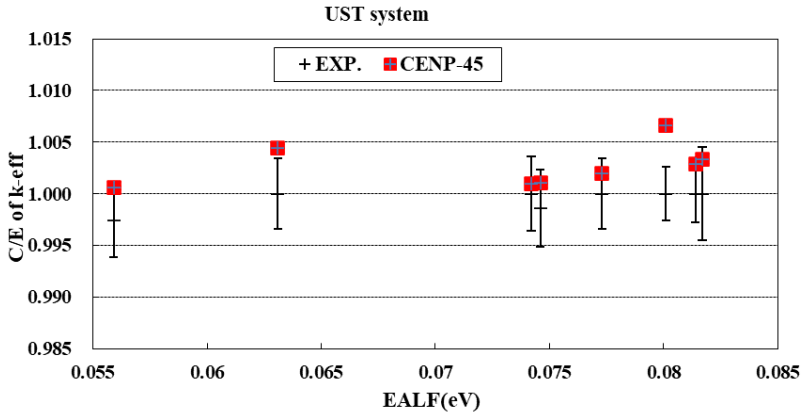

Figure 7 benchmark calculation results of UST system (EALF is in the range of 0.055 to 0.085eV)

4.3 burnup benchmark

bumup benchmark calculations have been performed for the JAEA benchmark problem which suite for reactor physics study of LWR next generation fuels [17] and Takahama-3 PWR spent fuel pin cell SF95[18]. the k_{inf} results of JAEA benchmark problem are showed in Figure 8-Figure 11.

The k-infinity results of the JAEA MOX pin cell are showed in Figure 8, the reference results were calculated by Monte Carlo and bumup code, k-infinity errors compared with reference results are provided in Figure 9. From Figure 9, we can find that the maximum errors of the simplified depletion chain are smaller than 250pcm.

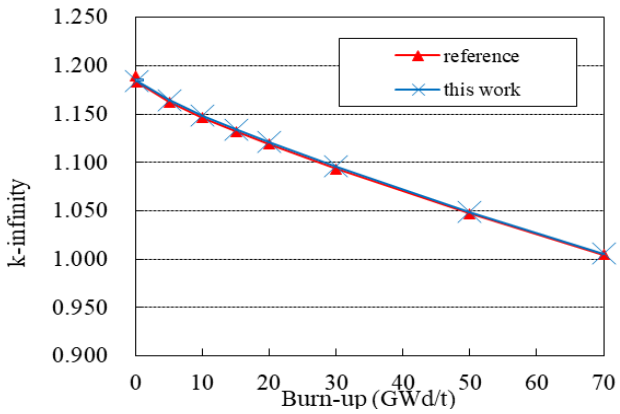

Figure 8 K-infinity results for MOX pin cell

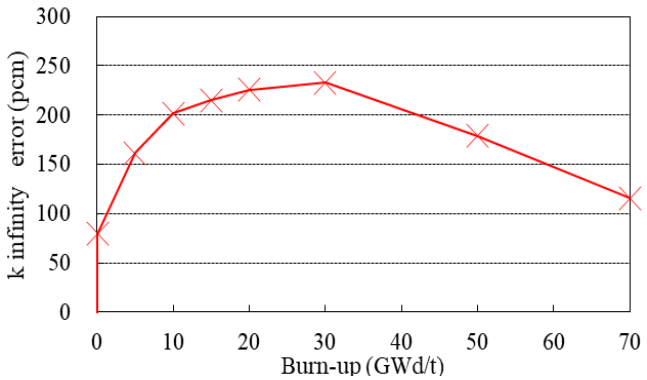

Figure 9 k-infinity error compared with reference results for MOX pin cell

The k-infinity results of the JAEA UO_2 pin cell are showed in Figure 10, k-infinity errors compared with reference results are provided in Figure 11. From Figure 11, we can find that the maximum errors of the simplified depletion chain are about 400pcm.

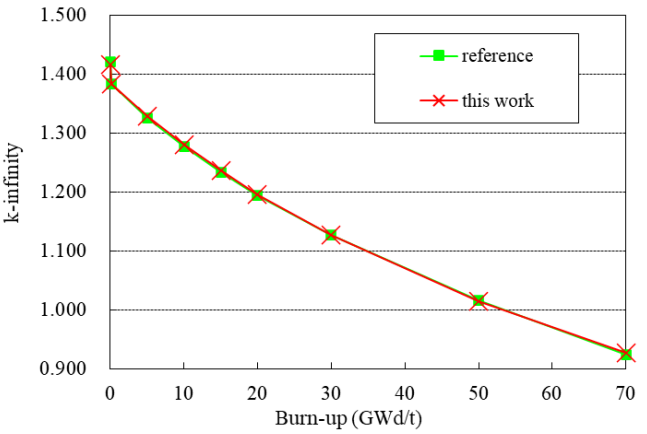

Figure 10 K-infinity results for UO_2 pin cell

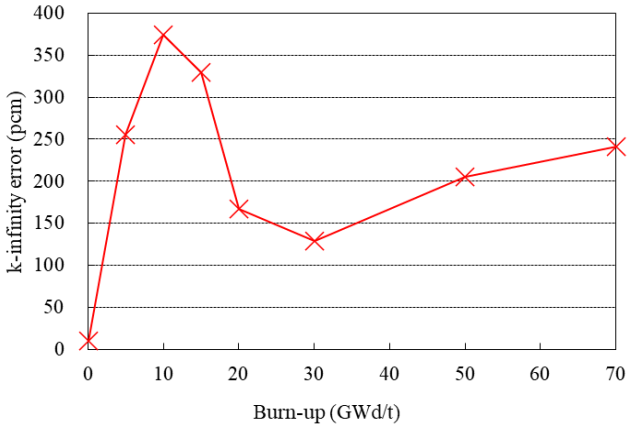

Figure 11 k-infinity error compared with reference results for UO_2 pin cell

AS to the benchmark calculation results of SF95, we mainly focus on the fission product nuclides. Accordingly, number densities of 20 nuclides are calculated and compared with results of the destructive analysis. The number density results of different sample are shown in Figure 12 -Figure 16.

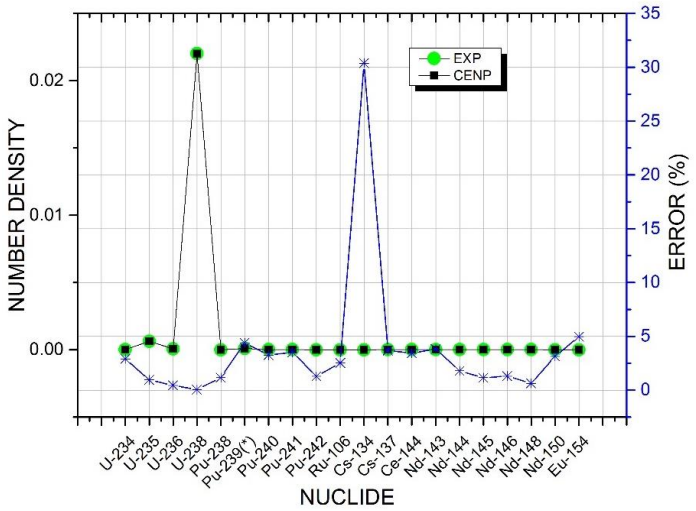

Figure 12 number density errors compared with experimental values for SF95-1 sample

In the calculation results of SF95-1 sample, except for the large error of Cs-134 (30.4%), the error of other nuclides is less than 5%.

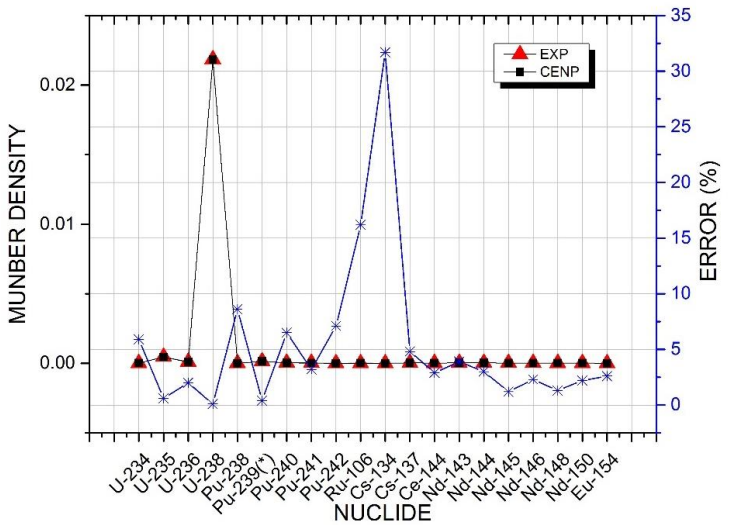

Figure 13 number density errors compared with experimental values for SF95-2 sample

In the calculation results of SF95-2 sample, Ru-106 and Cs-134 have such large error as 16.2% and 31.7%, the error of other nuclides is less than 8%, where most nuclides is less than 5%.

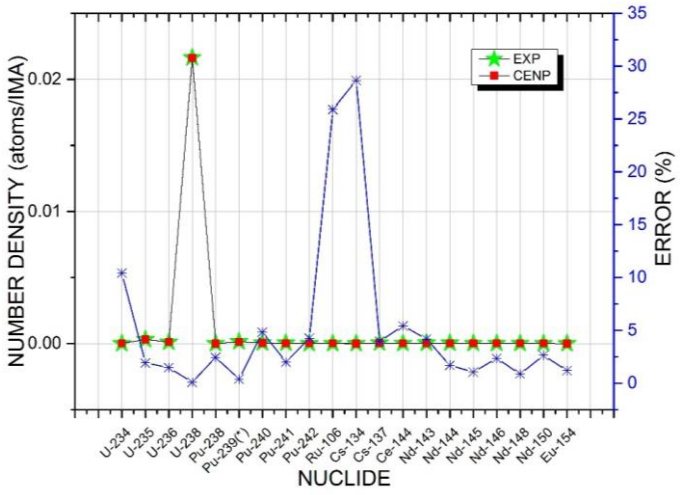

Figure 14 number density errors compared with experimental values for SF95-3 sample

In the calculation results of SF95-3, Ru-106 and Cs-134 have such large error as 25.9% and 28.7%, the error of U-234 is close to 10%, and the error of other nuclides is less than 5%.

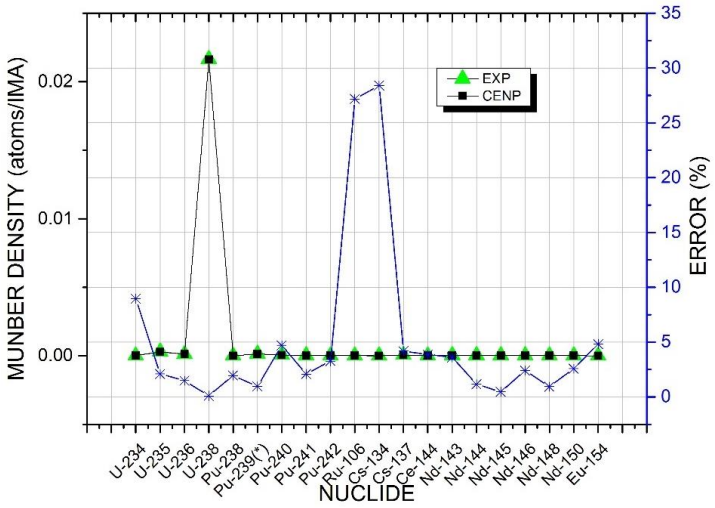

Figure 15 number density errors compared with experimental values for SF95-4 sample

The calculation results of SF95-4 are similar to those of SF95-3. Ru-106 and Cs-134 have large error more than 25%, the error of U-234 is close to 10%, and the error of other nuclides is no more than 5%.

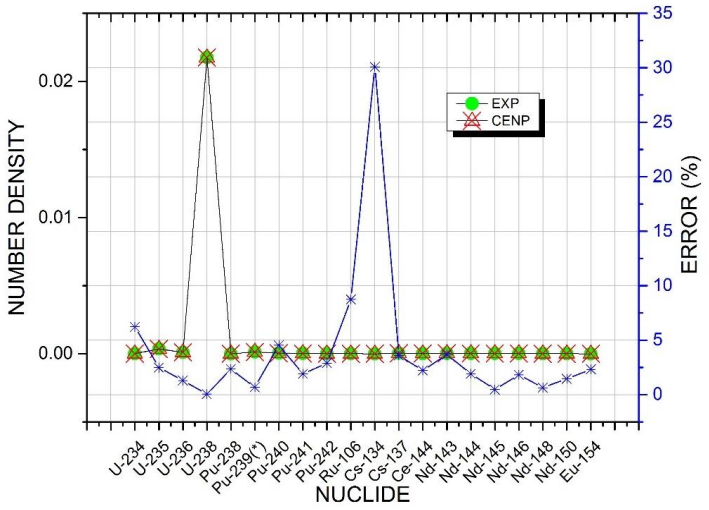

Figure 16 number density errors compared with experimental values for SF95-5 sample

In the calculation results of SF95-5, Cs-134 has large error, the error of Ru-106 is less than 10%, the error of U-234 is close to 5%, and the error of other nuclides is less than 5%.

The Monte Carlo code is used to model and calculate SF95. The results show that the errors between the MC calculated value of Ru-106 and the calculated value of Kylin-2 in this paper are 1.85% (SF95-1), 0.57% (SF95-2), 0.91% (SF95-3), 0.29% (SF95-4) and 0.35% (SF95-5) respectively. The calculated value of Ru-106 based on Helios program in reference [19] also deviates greatly from the experimental value, so it is suspected that the experimental value of Ru-106 is inaccurate. the large error of Cs-134 is considered to be caused by depletion chain which need to be further analyzed and improved. For other nuclides, the calculation error in this paper is significantly reduced compared with the calculation results of ORIGEN program and SWAT program in reference [18].

5. conclusion

In this paper a multigroup cross section library generation system named TPAMS was developed, the methods in TPAMS dealing with resonance data such as subgroup parameters, lambda factor, resonance integral were discussed. Moreover, the depletion chain simplification method was studied. TPAMS can produce multigroup library in binary and ASIIC formats, including detailed data contents for resonance, transport and depletion calculations. A multigroup cross section library has been generated for

KYLIN-2 based on TPAMS system. The multigroup cross section library was verified through the analysis of various criticality and burnup benchmarks, the values of multiplication factor and isotope density were compared with the experiment data. Numerical results demonstrate the accuracy of the multigroup cross section library and the reliability of the multigroup cross section library generation system TPAMS.

6. Reference:

[1] Chai Xiaoming, Tu Xiaolan, Lu Wei et al., 2017. The Powerful Method of Characteristics Module in Advanced Neutronics Lattice Code KYLIN-2. Journal of Nuclear Engineering and Radiation Science. Vol.3, 031004-1 - 031004-9.

[2] Hu Yuying, Liao Honghuan, Luo Qi et al., 2021. Study on an improved burnup algorithm in Kylin-2 code. Annals of Nuclear Energy. 153(2021) 108034,1-10.

[3] Pingzhou Ming, Junjie Pan, Xiaolan Tu et al.,2017. THE LINEAR SYSTEM SOLVER OF PROGRAMS NAMED CORTH AND KYLIN2. Proceedings of the 2017 25th International Conference on Nuclear Engineering, ICONE25. July 2-6, 2017, Shanghai, China.

[4] Nikolaev M N, Ignatov A A, Isaev n v, ET AL. The method of subgroups for considering the resonance structure of cross sections in neutron calculations[J]. Atomic Energy,1971,30(5):528-533.

[5] Hebert A, Coste M. Computing moment-based probability tables for self-shielding calculations in lattice codes[J]. Nuclear Science and Engineering, 2002,142(3):245-257.

[6] Lopez Aldama, R., Leszczynski, F., Trkov, A., 2003. WIMS-D Library Update, Final report of a coordinated research project. International Atomic Energy Agency.

[7] Katano, R., Yamamoto, A., Endo, T., 2014. Generation of Simplified Burnup Chain using Contribution Matrix of Nuclide Production. PHYSOR 2014, Kyoto, Japan, September 28-October 3.

[8] Takanori Kajihara, Masashi Tsuji, Go Chiba et al., 2014. Automatic Construction of a Simplified Burn-up Chain Model by the Singular Value Decomposition. PHYSOR 2014, Kyoto, Japan, September 28-October 3.

[9] Go Chiba, Masashi Tsuji, Tadashi Narabayashi, 2014. Important Fission Product Nuclide Identification method for Simplified Burnup Chain Construction. PHYSOR 2014, Kyoto, Japan, September 28-October 3.

[10] Huang Kai, Wu Hongchun, Li Yunzhao et al., 2016. Generalized Depletion Chain Simplification Based on Significance Analysis. PHYSOR2016, Sun Valley, America, May 1-6.

[11] Radha Thangaraj, Millie Pant, Ajith Abraham, A simple adaptive Differential Evolution algorithm. 2009 World Congress on Nature & Biologically Inspired Computing (NaBIC), 09-11 December 2009.

[12] CETNAR J. A method of transmutation trajectories analysis in accelerator driven system [R]. Proceedings of the IAEA Technical Committee Meeting on Feasibility and Motivation for Hybrid Concepts for Nuclear Energy Generation and Transmutation, Madrid, 17–19 September 1997.

[13] MACFARLANE, E.R., C.A. KAHLER AND W.D. MUIR, et al., The NJOY Nuclear Data Processing System, Version 2012[Report]. 2012: Los Alamos National Security.

[14] Sonzogni A.A., 2005. NuDa2.0: Nuclear Structure and Decay Data on the Internet. International Conference on Nuclear Data for Science and Technology.

[15] HERMAN, M. AND A. TRKOV, ENDF-6 Format Manual Data format and procedures for the Evuluated Nuclear Data File ENDF/B-VI and ENDF/B-VII[Report]. 2009, New York: Brookhaven National Laboratory.

[16] International Handbook of Evaluated Criticality Safety Benchmark Experiments, 2016. NEA/NSC/DOC (95)03/I-VIII. OECD NEA, Paris.

[17] Akio YAMAMOTO, Tadashi IKEHARA, Takuya ITO, Etsuro SAJI, 2002. Benchmark Problem Suite for Reactor Physics Study of LWR Next Generation Fuels. Journal of Nuclear Science and Technology, Vol.39, No.8, p.900-912.

[18] Yoshinori Nakahara, Kenya Suyama, Takenori Suzaki, 2002. Translation of Technical Development on Burn-up Credit for Spent LWR Fuels. Oak Ridge National Laboratory, JAERI-Tech 2000-071(ORNL/TR-2001/01).

[19] Isotopic Analysis of High-Burnup PWR Spent Fuel Samples from the Takahama-3 Reactor. Oak Ridge National Laboratory. NUREG/CR-6798, ORNL/TM-2001/259.